

By Jeremy Rowlette, Miles Weida, Benjamin Bird, David Arnone, Matthew Barre, and Timothy Day

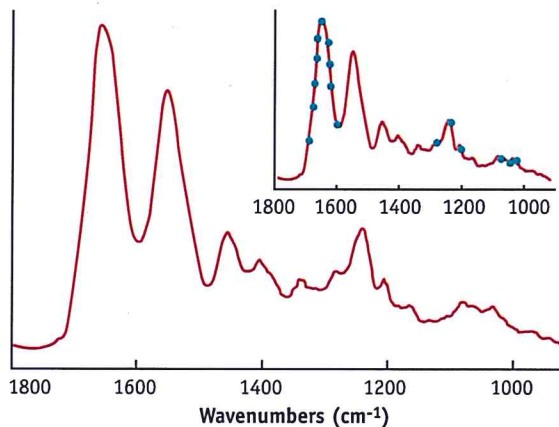
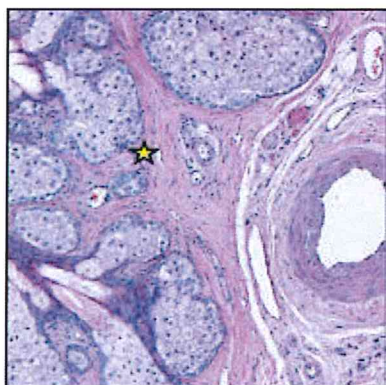
# High-confidence, high-throughput screening with high-def IR microspectroscopy

*High-definition infrared (IR) microspectroscopic imaging in a desktop system enables high-throughput cell and tissue screening for clinical diagnostics and drug discovery. Made possible by several technology advances, the system offers clinical pathology a bridge from traditional imaging to a new method that quantifiably assesses tissue for better diagnostic confidence.*

Current technologies used to classify excised clinical specimens—such as histology, cytology, immunohistochemistry (IHC), polymerase chain reaction (PCR), and DNA hybridization—have provided unquestionable benefit. But the accuracy of these techniques is compromised by such factors as small sample volume, affinity of stains and antibodies, and inter-observer variance. In addition, these techniques are restrictive because they can identify only targeted markers; there is no possibility for identification of unknown markers or disease variants.

## Enabling new paradigms

Over the past decade, a variety of spectroscopic techniques have been developed to provide rapid and sensitive



A representative single-pixel spectra collected from the eyelid tissue section shown in Fig. 4 shows high SNR and spectral fidelity. The inset illustrates the concept of the new sparse data collection modality.

characterization of relevant sample biochemistry. Because spectroscopic techniques are based on biochemical rather than morphological metrics, new diagnostic paradigms are thereby enabled. The adoption of infrared spectroscopic imaging (IR-SI) in biomedical

research is of particular note. In a rapidly expanding field, numerous high-quality investigations have highlighted a unique ability to identify early disease states, predictive molecular markers, and drug-resistant populations.

IR-SI produces detail-rich absorbance contrast image cubes (2D images with an IR spectral response at each pixel) of cells and tissue without requiring molecular labels, stains, or high optical power densities. Thus, IR-SI is especially suitable for studies on live cells.<sup>1</sup>

JEREMY ROWLETTE and MILES WEIDA are senior scientists, BENJAMIN BIRD is an application scientist, DAVID ARNONE is mechanical engineer, MATTHEW BARRE is business development manager, and TIMOTHY DAY is CEO at Daylight Solutions (San Diego, CA; [www.daylightsolutions.com](http://www.daylightsolutions.com)). Contact Mr. Barre at [mbarre@daylightsolutions.com](mailto:mbarre@daylightsolutions.com).



In a process referred to as digital staining, these image cubes may be further reduced into 2D biochemically differentiated maps using robust supervised-classification algorithms developed over the past decade.<sup>2-6</sup> Digital staining gives the pathologist or drug developer a powerful visual tool for quickly identifying subtle changes in the biochemical distribution of the sample, and may be used to enhance contrast between healthy

and diseased tissue or for screening of drug effects in tissue microarrays. This technique may prove particularly beneficial in detecting early stages of disease before visible morphological changes are present. Applications for this technology are growing rapidly and it is already making significant impact in the fields of cytology, histology, surgical pathology, structural microbiology, drug discovery, and stem cell research.<sup>1-5</sup>

Fourier transform infrared (FTIR) spectroscopic imaging microscopes using extended globar thermal light sources and HgCdTe (MCT) focal-plane arrays (FPAs) with pixel densities up to 128 × 128 are now available. However, their ability to rapidly collect high-spatial resolution spectral cubes over large areas while maintaining single-pixel signal-to-noise ratio (SNR) levels greater than 100:1 is limited by the inherently low spectral brightness of the globar source. IR radiation from large-scale (>10 m diameter) synchrotrons located at national research labs have been successfully combined with FTIR systems to greatly improve image quality and throughput, but the approach is impractical for meeting clinical and industrial needs.<sup>7</sup>

Furthermore, FTIR-based systems are governed by a fundamental trade-off between spectral resolution and spectral range. That is, signal must be acquired over a wide band to achieve

high resolution, even when absorption features are sparsely distributed over the collection range. Finally, FTIR-based systems do not provide live high-definition, full-field absorbance contrast imaging—though it is a modality

with tremendous potential in rapid screening applications.

Increased sample throughput, improved image quality, and smaller instruments are all needed to fully realize IR-SI technology in clinical

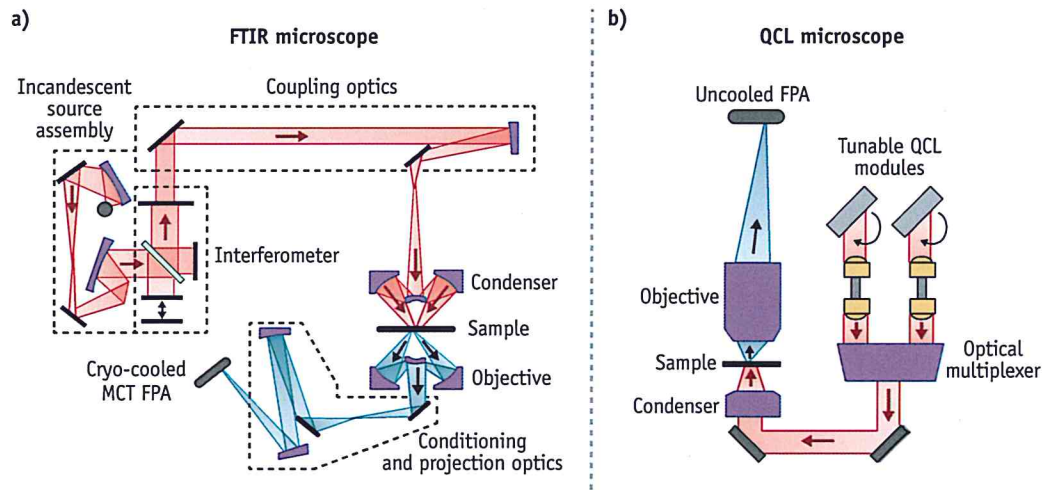


FIGURE 1. Schematics demonstrate the setups of a typical FTIR microscope (a) and a QCL IR-SI microscope (b).

## Make Conoptics Your Choice for

### Pulse Selection Systems

#### Specifications

- Select from a single shot to 30 mhz rep rate for mode locked lasers running as high as 100 mhz
- Low temporal dispersion compatible with FSECpulse; no spatial dispersion
- Optical, transmission >80%
- Available for TI: Sapphire and OPO's 700 to 1600nm

**Complete systems engineered to meet YOUR requirements.**

Phone: 800.748.3349  
 Fax: 203.790.6145  
 Email: sales@conoptics.com  
 Sales Reps World Wide  
 www.conoptics.com

**Electro-Optic Components & Systems**



diagnostic and pharmaceutical development labs.

**A desktop instrument**

To meet the demanding needs of clinical and pharmaceutical labs, the first high-definition, high-throughput, IR spectroscopic imaging desktop microscope marries a high-spectral-brightness, broadly tunable IR laser source with a large-format (480 × 480), uncooled microbolometer FPA camera. This instrument, produced by Daylight Solutions (San Diego, CA), achieves high-SNR, diffraction-limited, spectroscopic imaging over the 900–1800 cm<sup>-1</sup> molecular fingerprint region. It captures full spectral cubes within minutes or sparse data sets in seconds without the need for liquid nitrogen cooling. The main components of the quantum cascade laser (QCL)-based IR-SI microscope, as shown in Fig. 1, include multiple QCL modules, an optical multiplexer, a condenser, a switchable objective, an automated stage (not shown), and an uncooled microbolometer FPA. The architecture enables a small footprint, currently about one third that of a commercial FTIR microscope, and lends itself to further size reduction for mobile applications.

The laser source comprises multiple broadly tunable external cavity QCL modules that enable platform modularity and scalability. The high brightness of the QCL source takes advantage of the full dynamic range of commercial uncooled microbolometer FPAs having 14 times the number of pixels found in state-of-the-art FTIR microscopes (see Fig. 2). This dynamic range is >1000 for a single frame acquisition.

The instrument employs a family of novel, purpose-designed, high-numerical-aperture (NA), achromatic, wide-field, IR refractive objectives optimized for coherent IR microscopy in the molecular fingerprint region. This development disrupts the long-standing paradigm of Cassegrain objectives in IR spectroscopic

imaging, effectively removing the practical ceiling for numerical aperture that governs spatial resolution. The existing microscope embodiment has a three-position turret that is easily configured to meet application needs. The standard configuration of the microscope includes one visible and two IR objectives. One of the IR objectives currently available has an NA of 0.7 and a magnification of 12.5X. When combined with the 480 × 480 FPA, it achieves diffraction-limited resolution of 5 μm at 1650 cm<sup>-1</sup> (corresponding to the peak of a typical Amide I band), a sample-referred pixel size of 1.36 μm, and a field of view (FOV) of 650 μm. Tissue microarrays (TMA) with cores 0.6 mm in size, routinely used in research pathology, can be examined using a single field of view of the new IR microscope, allowing high-throughput screening at a definition never before available. Achieving the same pixel resolution on a high-end FTIR microscope using a 128 × 128 MCT FPA and a globar source would require a 60X objective.

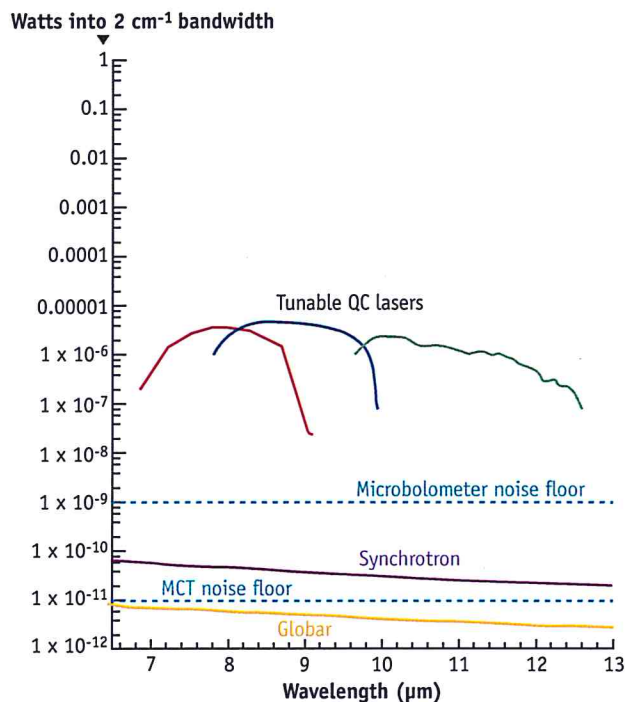


FIGURE 2. Spectral brightness of globars, synchrotron IR source, and QCL lasers over the 7–12 μm (833–1430 cm<sup>-1</sup>) range differ in relation to the noise floors of commercial MCT and microbolometer FPAs.

At this magnification, the FOV would only be 174 μm (~14X smaller viewing area than the IR microscope) and require a 4 × 4 stitched mosaic collection protocol. Getting similar SNR levels at this resolution and FOV, an FTIR microscope would require nearly a half-day for data collection.

Figure 3 shows a chrome-on-glass USAF 1951 resolution target, imaged in reflection mode with the 0.7 NA, 12.5X objective at 1555 cm<sup>-1</sup>, shows

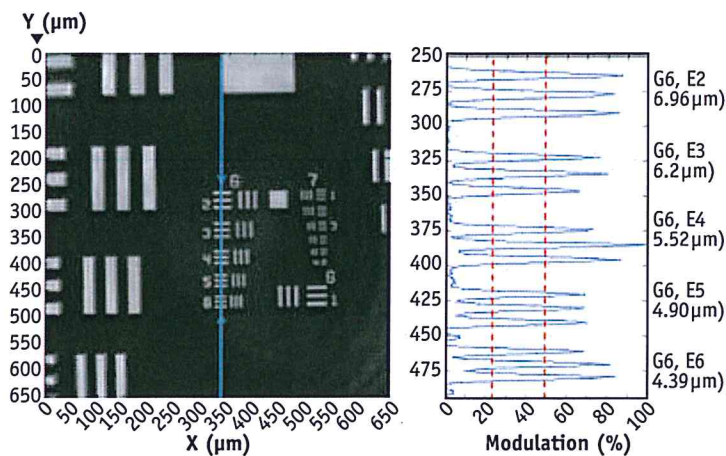
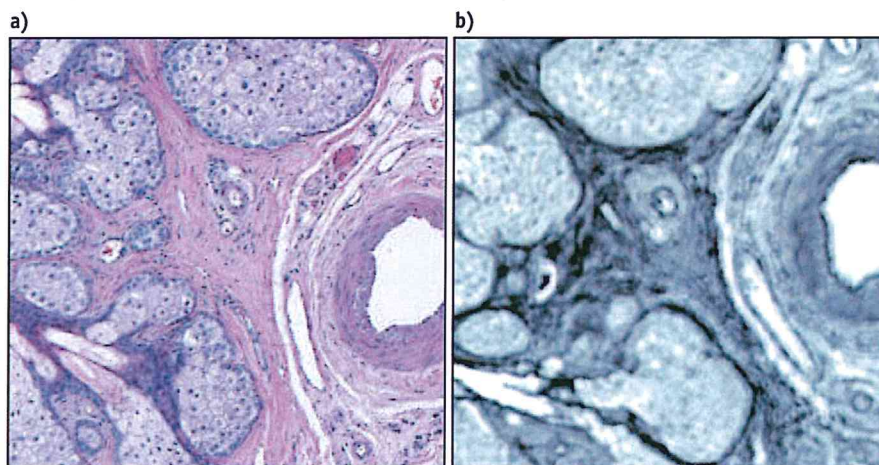


FIGURE 3. In a reflectance image of Groups 6 and 7 of a chrome-on-glass USAF 1951 resolution test target—collected with the IR microscope using the 0.7 NA, 12.5X objective at 1555 cm<sup>-1</sup> in reflection mode—the profile plot along Group 6 shows that the Rayleigh criteria is met for bars with spacing below 5 μm.





**FIGURE 4.** Different views of an eyelid tissue section containing a meibomian gland. The visible image (a) is an H&E stained section collected using a white light microscope. The absorbance image (b) is of a neighboring unstained section of the same tissue location fixed to CaF<sub>2</sub> disk and was collected by the IR microscope at 1650 cm<sup>-1</sup> using the 0.7 NA, 12.5X objective in transmission mode.

that the Rayleigh criterion for diffraction-limited performance is achieved for bars with spacing below 5  $\mu\text{m}$ . Figure 4 shows an absorbance contrast image of a 5- $\mu\text{m}$ -thick unstained tissue section of an eyelid containing a meibomian gland that has been fixed to a CaF<sub>2</sub> disk. This image was taken with the 0.7 NA, 12.5X IR objective at 1650 cm<sup>-1</sup> in transmission mode. Cellular boundaries and nuclei are resolvable while simultaneously viewing a full 650  $\mu\text{m}$  field.

The standard microscope configuration also includes an ultra-wide-field 4X IR objective with 2 mm FOV and a sample-referred pixel size of 4.25  $\mu\text{m}$ . This objective is especially useful in rapidly surveying large areas of tissue sections or in the simultaneous imaging of multiple 0.6 mm TMA cores (a 2  $\times$  2 array of 0.6 mm TMA cores with standard spacing can be observed). Once an area of interest has been identified, it is straightforward to transition to the 0.7 NA, 12.5X objective and perform detailed spectroscopic imaging.

The Frontis image demonstrates the representative quality (spectral fidelity and SNR) of single-pixel spectra collected from the eyelid tissue section shown in Fig. 4. Here, the Amide I and II protein bands, as well as the classic triad of bands in the low-wavenumber region, associated with collagen in fibroconnective tissue, are clearly

present and in accordance with FTIR measurements.

#### New modalities

The IR microscope is also capable of live, discrete-frequency, chemical imaging at a 30 Hz frame rate, a mode well suited for intra-operative tumor screening of frozen tissue sections, live cell studies, and multiplexed chemotyping. Further, the IR microscope can tune to arbitrary frequencies within the 900–1800 cm<sup>-1</sup> band on demand or in a user-defined, non-uniformly spaced vector, enabling a fast, sparse data collection mode. This mode may be used to greatly increase data acquisition speeds and enable large-scale multiplexed screening applications where key spectral features can be targeted. For example, a dense set of spectral points may be clustered around broad spectral bands (such as protein bands) to detect small changes in band area, centroid, or shape, whereas sharp bands may require only a small number of points to detect the presence or absence of targeted chemical absorption markers. The inset in the Frontis illustrates the concept of performing a user-defined sparse data collection.

#### The path to clinical diagnostics

Today, pathologists routinely use real-time visible white light microscopy of

hematoxylin and eosin (H&E)-stained specimens to ascertain the presence and extent of disease. Because they are not typically trained in histochemical vibrational spectroscopy, they are not likely to readily adopt instruments providing only spectroscopic image cubes.

Real-time, high-definition IR absorbance imaging microscopy can bridge the gap between spectral pathology research and clinical pathology: Pathologists can use the live imaging capability, much as they do with visible light microscopy, to quickly screen large sections of tissue, perhaps moving back and forth between a handful of discrete frequencies to enhance chemical image contrast. Once the clinical pathologist has identified a region of interest, a full spectral cube can be collected quickly, while supervised chemical classification algorithms can provide deeper insight into subtle histochemical changes. The result is a high-confidence diagnosis.

This new paradigm injects new hope into the quest for earlier detection, more accurate diagnosis, and faster treatment of disease. <<

#### ACKNOWLEDGEMENTS

We would like to thank Prof. Nora M. V. Laver (Tufts University School of Medicine) for providing high-quality eyelid tissue sections on CaF<sub>2</sub> disks, and Prof. Michael Walsh (University of Illinois at Chicago, Department of Pathology) for providing a variety of high-quality tissue sections on CaF<sub>2</sub> disks.

#### REFERENCES

1. L. Chen et al., *Anal. Chem.*, 84, 4118–4125 (2012).
2. P. Heraud and B. Wood (Eds.), *Analyt.*, 138, 14, 3847–4204 (2013).
3. C. Krafft and B. Bird (Eds.), *J. Biophoton.*, 6, 1, 1–121 (2013).
4. B. Bird et al., *Lab. Invest.*, 92, 1358–1375 (2012).
5. M. J. Walsh, R. K. Reddy, and R. Bhargava, *IEEE J. Sel. Topics Quantum Electron.*, 18, 1502–1513 (2012)
6. J. Cao et al., *Int. J. Mol. Sci.*, 14, 17453–17476 (2013).
7. M. J. Nasse et al., *Nat. Meth.*, 8, 413–416 (2011).